

## Scattering and Imaging with Diffusing Temporal Field Correlations

D. A. Boas,\* L. E. Campbell,† and A. G. Yodh

*Department of Physics, University of Pennsylvania, Philadelphia, Pennsylvania 19104*  
(Received 12 May 1995)

We consider the transport of the electric field temporal autocorrelation in *heterogeneous*, fluctuating turbid media. Experiments are performed in strongly scattering media with spatially separated static and dynamic components, and low resolution “dynamical” images of such media are obtained using autocorrelation measurements of the emerging speckle fields taken along the sample surface. Our analysis, based on a diffusion approximation to the field correlation transport equation, reveals that the field correlation scatters from macroscopic dynamical heterogeneities within turbid media.

PACS numbers: 82.70.Dd, 82.70.Kj, 82.70.Rr, 87.59.-e

For many years dynamical information about materials has been extracted from the temporal fluctuations of scattered light fields. Most experiments of this nature [1] are carried out in optically thin materials that scatter incident photons no more than once. More recently there has arisen a growing interest in the properties of diffusing light fields emerging from turbid media [2–4]. A particularly robust example of these developments is the technique of diffusing-wave spectroscopy (DWS) [3,4], where the temporal correlation functions of diffuse speckle fields have provided new information about fundamental motions in *homogeneous* turbid colloids [5], foams [6], and emulsions [7]. Thus far, DWS has only been considered in the context of uniform, strongly scattering media. Clearly it is desirable to probe turbid media possessing more complex structures. For example, in the biophysics community simpler properties of diffusing photons, such as the refraction and diffraction of diffuse photon density waves, are now used to generate low resolution images of static absorption and scattering variations within heterogeneous tissues [2].

In this paper we consider the diffusion of the temporal field correlation itself through *heterogeneous* turbid media. We show that the transport of diffusive temporal field correlation through a medium consisting of spatially distinct static and dynamic parts can be viewed as a scattering process, and we experimentally demonstrate that position-dependent measurements of the diffusing light field temporal autocorrelation function can be used to reconstruct images of the spatial variation of *dynamical* properties within the medium. Besides its intrinsic interest as a new phenomenon, the scattering of diffusive temporal field correlation offers an unexplored contrast mechanism for imaging within heterogeneous turbid media such as tissue, and provides experimenters with a better framework for the interpretation of correlation functions from more complex, spatially heterogeneous colloids, foams, and emulsions.

The theoretical basis of our approach may be derived from the linear transport equation for field correlation recently presented by Ackerson *et al.* [8] or by field theoretic methods [3]. Both methods are valid for scalar fields. Within the  $P_1$  approximation [9–11], the correlation trans-

port equation reduces to the following steady-state diffusion equation for field correlation in homogeneous turbid media such as a dense colloid,

$$(-D_\gamma \nabla^2 + v\mu_a + 2vD_B k_0^2 \tau / l^*) G_1(\mathbf{r}, \tau) = S(\mathbf{r}). \quad (1)$$

Here  $G_1(\mathbf{r}, \tau) = \langle E(\mathbf{r}, t) E^*(\mathbf{r}, t + \tau) \rangle$  is the unnormalized temporal electric field autocorrelation function at the position  $\mathbf{r}$  within the sample,  $D_\gamma = vl^*/3$  is the *photon diffusion coefficient* within the sample,  $l^*$  is the photon random walk step,  $\mu_a$  is the absorption coefficient, and  $v$  is the speed of light in the medium. The  $\langle \dots \rangle$  denote an ensemble average or, in the case of an ergodic system, an average over time  $t$ .  $D_B$  is the *particle diffusion coefficient* within the medium,  $k_0$  is the wave number of the light in the medium, and  $\tau$  is the correlation time. The source light distribution is given by  $S(\mathbf{r})$ . Equation (1) is expressed equivalently as the diffusion pole of the two point correlation function of the light electric field in Ref. [3].

Before introducing the experiment we briefly discuss two simple solutions to Eq. (1). We first observe that Eq. (1) can be recast as a Helmholtz equation for the field correlation function, i.e.,

$$[\nabla^2 + K^2(\tau)] G_1(\mathbf{r}, \tau) = -\frac{S}{D_\gamma} \delta^3(\mathbf{r} - \mathbf{r}_s), \quad (2)$$

where  $K^2(\tau) = -v(\mu_a + 2D_B k_0^2 \tau / l^*) / D_\gamma$ . Here we have taken the light source to be pointlike, and located at position  $\mathbf{r}_s$ . Note that  $2D_B k_0^2 \tau / l^*$  is a loss term similar to  $\mu_a$ . While  $\mu_a$  represents losses due to photon absorption,  $2D_B k_0^2 \tau / l^*$  represents the “absorption” of correlation due to dynamic processes. When  $\tau = 0$  there is no dynamic absorption and Eq. (2) reduces to the steady-state photon diffusion equation [2].

For an infinite, homogeneous system with no photon absorption (i.e.,  $\mu_a = 0$ ), the solution to Eq. (2) has the well known form  $G_1(\mathbf{r}, \tau) = S \exp(-\sqrt{6D_B k_0^2 \tau / l^*} |\mathbf{r} - \mathbf{r}_s|) / 4\pi D_\gamma |\mathbf{r} - \mathbf{r}_s|$ . The same solution has been derived from the scalar wave equation for the electric field propagating in a medium with a fluctuating dielectric constant [3], and within the context of diffusing-wave spectroscopy [4]. In contrast to these two approaches, the correlation

diffusion equation provides a simple framework for considering turbid media with large scale *spatially varying dynamics*, that is, media where  $D_B = D_B(\mathbf{r})$ .

The second simple solution is for a medium which is homogeneous in all respects except for a spherical region (with radius  $a$ ) characterized by a different value of  $D_B$  than the surrounding medium. The analytic solution of the correlation diffusion equation for this system reveals that the measured correlation function outside the sphere can be interpreted as a superposition of the incident correlation plus a term which accounts for the scattering of the correlation from the sphere, i.e.,

$$G_1^{\text{out}}(\mathbf{r}_s, \mathbf{r}_d, \tau) = \frac{S \exp[iK^{\text{out}}(\tau) |\mathbf{r}_d - \mathbf{r}_s|]}{4\pi D_y |\mathbf{r}_d - \mathbf{r}_s|} + \sum_{l=0}^{\infty} A_l H_l^{(1)}(K^{\text{out}} r_d) Y_l^0(\theta, \phi). \quad (3)$$

Here,  $H_l^{(1)}$  are Hankel functions of the first kind and  $Y_l^0(\theta, \phi)$  are spherical harmonics [12]. The coefficient  $A_l$  is the scattering amplitude of the  $l$ th partial wave and is found by matching the appropriate boundary conditions on the surface of the sphere [13]. This solution has been discussed in detail for diffuse photon density waves [14]. By viewing the perturbation of temporal correlation as a scattering process, simple algorithms adapted from scattering theory can be applied to reconstruct images of spatially varying dynamics in turbid media.

We demonstrate the scattering of temporal correlation by a dynamical inhomogeneity in an experiment shown in Fig. 1. In this experiment, the temporal intensity correlation function is measured in remission from a semi-infinite, highly scattering, solid slab of  $\text{TiO}_2$  suspended in resin ( $D_B = 0$ ). The slab contains a spherical cavity filled with a turbid, fluctuating suspension of  $0.296 \mu\text{m}$

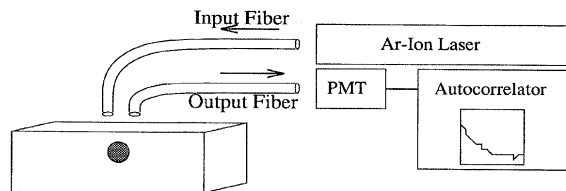


FIG. 1. The 514 nm line from an argon ion laser (operated at 2.0 W with an etalon) is coupled into a multimode fiber optic cable and delivered to the surface of a solid slab of  $\text{TiO}_2$  suspended in resin. The slab has dimensions of  $15 \times 15 \times 8$  cm. A spherical cavity with a diameter of 2.5 cm is located 1.8 cm below the center of the upper surface. The cavity is filled with a 0.2% suspension of  $0.296 \mu\text{m}$  diameter polystyrene spheres at  $25^\circ\text{C}$  resulting in  $l^* = 0.15$  cm,  $\mu_a = 0.002 \text{ cm}^{-1}$ , and  $D_B = 1.5 \times 10^{-8} \text{ cm}^2/\text{s}$ . For the solid,  $l^* = 0.22$  cm and  $\mu_a = 0.002 \text{ cm}^{-1}$ . A single-mode fiber collects light at a known position and delivers it to a photomultiplier tube (PMT), whose output enters a digital autocorrelator to obtain the temporal intensity correlation function. The temporal intensity correlation function is related to the temporal field correlation function by the Siegert relation [4]. The fibers can be moved to any position on the sample surface.

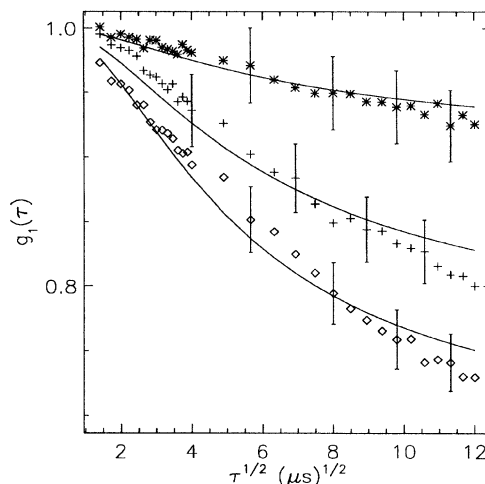


FIG. 2. Experimental measurements of the normalized temporal field autocorrelation function for three different source-detector pairs are compared with theory. With respect to an  $x$ - $y$  coordinate system whose origin lies directly above the center of the spherical cavity, the source-detector axis was aligned parallel to the  $y$  axis with the source at  $y = 1.0$  cm and the detector at  $y = -0.75$  cm. Keeping the source-detector separation fixed at 1.75 cm, measurements were made at  $x = 0.0, 1.0,$  and  $2.0$  cm, and are indicated by the  $\diamond$ 's,  $+$ 's, and  $*$ 's, respectively. The uncertainty for these measurements is 3% and arises from uncertainty in the position of the source and detector. The solid line was calculated using the known experimental parameters (see Fig. 1). Note that larger and more rapid decays are observed when the source and detector are nearest the dynamic sphere. Here the largest fraction of detected photons have sampled the dynamic region.

polystyrene balls ( $D_B = 1.5 \times 10^{-8} \text{ cm}^2/\text{s}$ ) [15]. In Fig. 2 we plot the measured decay of the normalized temporal field correlation function,  $g_1(\tau) = \langle E(t)E^*(t + \tau) \rangle / \langle |E|^2 \rangle$ , for different source-detector positions and compare these results to theoretical predictions based on Eq. (3). The agreement between experiment and theory is good, supporting our view that correlation "scatters" from spatial variations of the particle diffusion coefficient  $[D_B(\mathbf{r})]$  within the medium. In general, correlation will scatter from spatial variations in the absorption  $[\mu_a(\mathbf{r})]$ , the photon random walk step  $[l^*(\mathbf{r})]$ , and the dynamic  $[D_B(\mathbf{r})]$  properties of turbid media.

Since the perturbation of correlation by inhomogeneities can be viewed as a scattering process, one can envision the application of tomographic algorithms for the reconstruction of images of spatially varying dynamics [16]. We have investigated this possibility. Our inversion algorithm, one of several possible schemes [16,17], is based on a solution to the correlation diffusion equation, Eq. (1), generalized to include spatially varying dynamics, i.e.,  $D_B = D_B(\mathbf{r})$ . For simplicity, we assume here that the medium has homogeneous  $l^*$  and  $\mu_a$ . We seek a solution of the form  $G_1(\mathbf{r}_s, \mathbf{r}_d, \tau) = G_1^0(\mathbf{r}_s, \mathbf{r}_d, \tau) \times \exp[\Phi_s(\mathbf{r}_s, \mathbf{r}_d, \tau)]$ , where  $G_1^0(\mathbf{r}_s, \mathbf{r}_d, \tau)$  is the solution of the

correlation diffusion equation in the absence of dynamical heterogeneities and  $\Phi_s(\mathbf{r}_s, \mathbf{r}_d, \tau)$  accounts for the effects of the presence of those heterogeneities. Within the Rytov approximation [17], we obtain an integral equation relating  $\Phi_s(\mathbf{r}_s, \mathbf{r}_d, \tau)$  to the spatial variation of  $D_B$ , i.e.,

$$\Phi_s(\mathbf{r}_s, \mathbf{r}_d, \tau) = - \frac{6k_0^2 \tau}{l^{*2} G_1^0(\mathbf{r}_s, \mathbf{r}_d, \tau)} \times \int d^3 r' H(\mathbf{r}', \mathbf{r}_d, \tau) G_1^0(\mathbf{r}_s, \mathbf{r}', \tau) \delta D_B(\mathbf{r}'). \quad (4)$$

Here,  $H(\mathbf{r}', \mathbf{r}_d, \tau)$  is the Green's function for the homogeneous correlation diffusion equation and  $\delta D_B(\mathbf{r})$  represents the spatial variation in the particle diffusion coefficient relative to the background value. The position of the source (detector) is  $\mathbf{r}_s$  ( $\mathbf{r}_d$ ).

In Fig. 3 we present an experimental image of  $D_B(\mathbf{r})$ . There are many techniques that can be employed to invert Eq. (4) [16,17]. Our image of  $D_B(\mathbf{r})$  was reconstructed from  $\sim 600$  measurements of the scattered correlation function,  $U_s(\mathbf{r}_s, \mathbf{r}_d, \tau)$ , using 400 iterations of the simultaneous iterative reconstruction technique [17]. The sample medium consisted of a solid cylinder of  $\text{TiO}_2$  suspended in resin. The cylinder was homogeneous except for a 1.3 cm diameter spherical cavity which was filled with an aqueous suspension of  $0.296 \mu\text{m}$  polystyrene balls and centered at  $z = 0$  (the  $z$  axis is the axis of the cylinder). Measurements were made every  $30^\circ$  at the surface of the cylinder for  $z = 0, 1, \text{ and } 2 \text{ cm}$ , with source-detector angular separations of  $30^\circ$  and  $170^\circ$  and correlation times of  $\tau = 15, 25, 35, 45, 55, 65, 75, \text{ and } 85 \mu\text{s}$ . The  $z = 0$  slice of the image is shown in Fig. 3(b). From this image the center (in the  $x$ - $y$  plane) of the dynamic region and the magnitude of the particle diffusion coefficient are determined. The center of the object in the image is within 2 mm of the actual center of the dynamic sphere. This discrepancy scales with the uncertainty in the position of the source and detec-

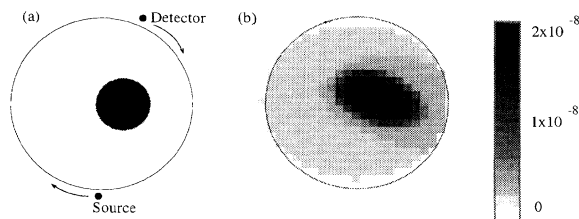


FIG. 3. An image reconstructed from experimental measurements of the scattered correlation function is shown in (b). The system was a 4.6 cm diameter cylinder with  $l^* = 0.25 \text{ cm}$ ,  $\mu_a = 0.002 \text{ cm}^{-1}$ , and  $D_B = 0$  [see illustration in (a)]. A 1.3 cm diameter spherical cavity was centered at  $x = 0.7 \text{ cm}$ ,  $y = 0$ , and  $z = 0$  and filled with a colloid with  $l^* = 0.25 \text{ cm}$ ,  $\mu_a = 0.002 \text{ cm}^{-1}$ , and  $D_B = 1.5 \times 10^{-8} \text{ cm}^2/\text{s}$ . A slice of the image at  $z = 0 \text{ cm}$  is presented in (b). The values of the reconstructed particle diffusion coefficients are indicated by the legend in units of  $\text{cm}^2/\text{s}$ .

tor. The sphere diameter ( $\sim 1.3 \text{ cm}$ ) and particle diffusion coefficient ( $\sim 1.8 \times 10^{-8} \text{ cm}^2/\text{s}$ ) obtained from the imaging procedure also agree reasonably well with experimentally known parameters (1.3 cm and  $1.5 \times 10^{-8} \text{ cm}^2/\text{s}$ ).

The calculations and experiments described thus far demonstrate the diffusion and scattering of correlation in turbid samples where the dynamics are governed by Brownian motion. The correlation diffusion equation can be modified to account for other dynamical processes as well, such as shear flow and random flow. In the case of random particle flow,  $K^2(\tau)$  is decreased by an additional factor  $k_0^2 \langle V^2 \rangle \tau^2 / l^{*2}$ , where  $\langle V^2 \rangle$  is the second moment of the particle speed distribution (assumed Gaussian) [18]. Flow in turbid media is an interesting problem that has received some attention. In these measurements experimenters typically determine a correlation function that may be a compound of many decays representing a weighted average of flow within the sample. For example, Bonner and Nossal have developed an approach for measuring random blood flow in homogeneous tissue [18], Wu *et al.* have applied DWS to study uniform shear flow [19], and Bicout and co-workers have applied DWS to study inhomogeneous flow and turbulence [20]. In all cases, *a priori* knowledge of the flow is used in the analyses. We expect that the application of correlation diffusion imaging will further clarify information about heterogeneous flows in turbid media.

In conclusion, we have shown that the transport of temporal correlation through heterogeneous turbid media can be viewed as a scattering of diffuse correlation. This concept has been demonstrated experimentally in the context of both forward and inverse problems. We anticipate these observations will stimulate further studies of dynamical variations in heterogeneous complex fluids. In medical optical imaging this approach offers another contrast mechanism for the identification of calcified tumors, skeletal structures, ischemia, and blood flow.

The authors thank Maureen O'Leary for assistance with the image reconstructions and insightful comments, and acknowledge illuminating conversations with Britton Chance and David Pine. A. G. Y. acknowledges partial support from the NSF through the P.Y.I. program and Grant No. DMR93-06814, and the Alfred P. Sloan Foundation.

\*Also with the Department of Biophysics and Biochemistry, University of Pennsylvania, Philadelphia, PA 19104.

†On leave from the Department of Physics, Hobart and William Smith Colleges, Geneva, NY 14456.

- [1] R. Pecora, in *Dynamic Light Scattering: Applications of Photon Correlation Spectroscopy* (Plenum Press, New York, 1985).
- [2] See A. Yodh and B. Chance, *Phys. Today* **10**, No. 3, 34 (1995), and references therein.

- [3] M. J. Stephen, Phys. Rev. B **37**, 1 (1988); F. C. MacKintosh and S. John, Phys. Rev. B **40**, 2382 (1989).
- [4] D. J. Pine, D. A. Weitz, P. M. Chaikin, and E. Herbolzheimer, Phys. Rev. Lett. **60**, 1134 (1988); G. Maret and P. E. Wolf, Z. Phys. B **65**, 409 (1987).
- [5] X. Qiu *et al.*, Phys. Rev. Lett. **65**, 516 (1990); P. D. Kaplan, A. G. Yodh, and D. J. Pine, Phys. Rev. Lett. **68**, 393 (1992); J. X. Zhu *et al.*, Phys. Rev. Lett. **68**, 2559 (1992); M. H. Kao, A. G. Yodh, and D. J. Pine, Phys. Rev. Lett. **70**, 242 (1993); S. J. Nilsen and A. P. Gast, J. Chem. Phys. **101**, 4975 (1994); A. J. C. Ladd, H. Gang, J. X. Zhu, and D. A. Weitz, Phys. Rev. Lett. **74**, 318 (1995).
- [6] D. J. Durian, D. A. Weitz, and D. J. Pine, Science **252**, 686 (1991).
- [7] H. Gang, A. H. Krall, and D. A. Weitz, Phys. Rev. Lett. **73**, 3435 (1994); P. D. Kaplan, A. G. Yodh, and D. F. Townsend, J. Colloid Interface Sci. **155**, 319 (1993).
- [8] B. J. Ackerson, R. L. Dougherty, N. M. Reguigui, and U. Nobbman, J. Thermophys. Heat Trans. **6**, 577 (1992); R. L. Dougherty *et al.*, J. Quant. Spectrosc. Radiat. Transfer **52**, 713 (1994).
- [9] K. M. Case and P. F. Zweifel, in *Linear Transport Theory* (Addison-Wesley, Reading, MA, 1967).
- [10] S. Glasstone and M. C. Edlund, in *The Elements of Nuclear Reactor Theory* (D. van Nostrand Co., Princeton, NJ, 1952).
- [11] In general the  $P_1$  approximation assumes that the correlation at a given point in space is nearly isotropic. This is a valid assumption when the photons are diffusing. We make the additional assumption that the correlation time is small compared to the time it takes a scattering particle to move a wavelength of light.
- [12] The sphere is centered on the origin, and the source is placed on the  $z$  axis to exploit azimuthal symmetry.
- [13] The boundary conditions are  $G_1^{\text{out}}(a, \tau) = G_1^{\text{in}}(a, \tau)$  and  $-D_\gamma^{\text{out}} \hat{n} \cdot \nabla G_1^{\text{out}}(a, \tau) = -D_\gamma^{\text{in}} \hat{n} \cdot \nabla G_1^{\text{in}}(a, \tau)$  on the surface of the sphere, where  $G_1^{\text{in}}(\mathbf{r}, \tau)$  is the correlation function inside the spherical object and  $\hat{n}$  is the normal vector to the sphere.
- [14] D. A. Boas, M. A. O'Leary, B. Chance, and A. G. Yodh, Proc. Natl. Acad. Sci. U.S.A. **91**, 4887 (1994); P. N. den Outer, T. M. Nieuwenhuizen, and A. Lagendijk, J. Opt. Soc. Am. A **10**, 1209 (1993).
- [15] Because of the nonergodic nature of the system, it was necessary to ensemble average the correlation function by translating the sample over a 400  $\mu\text{m}$  region during each measurement of the correlation function. See J. Xue *et al.*, Phys. Rev. A **46**, 6550 (1992), for further discussion of this procedure.
- [16] See related works by S. R. Arridge *et al.*, J. P. Kaltenbach *et al.*, and R. L. Barbour *et al.*, in the volume *Medical Optical Tomography: Functional Imaging and Monitoring*, edited by G. Muller *et al.* (SPIE Optical Engineering Press, Bellingham, WA, 1993), Vol. 1s11, pp. 31–143.
- [17] A. C. Kak and M. Slaney, in *Principles of Computerized Tomographic Imaging* (IEEE Press, New York, 1988); M. A. O'Leary, D. A. Boas, B. Chance, and A. G. Yodh, Opt. Lett. **20**, 426 (1995).
- [18] R. Bonner and R. Nossal, Appl. Opt. **20**, 2097 (1981).
- [19] X-L. Wu, D. J. Pine, P. M. Chaikin, J. S. Huang, and D. A. Weitz, J. Opt. Soc. Am. B **7**, 15 (1990).
- [20] D. Bicot and R. Maynard, Physica (Amsterdam) **199A**, 387 (1993); D. Bicot and G. Maret, Physica (Amsterdam) **210A**, 87 (1994); D. J. Bicot and R. Maynard, Physica (Amsterdam) **204B**, 20 (1995).

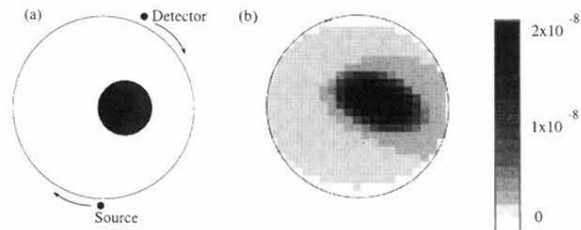


FIG. 3. An image reconstructed from experimental measurements of the scattered correlation function is shown in (b). The system was a 4.6 cm diameter cylinder with  $l^* = 0.25$  cm,  $\mu_a = 0.002$  cm $^{-1}$ , and  $D_B = 0$  [see illustration in (a)]. A 1.3 cm diameter spherical cavity was centered at  $x = 0.7$  cm,  $y = 0$ , and  $z = 0$  and filled with a colloid with  $l^* = 0.25$  cm,  $\mu_a = 0.002$  cm $^{-1}$ , and  $D_B = 1.5 \times 10^{-8}$  cm $^2$ /s. A slice of the image at  $z = 0$  cm is presented in (b). The values of the reconstructed particle diffusion coefficients are indicated by the legend in units of cm $^2$ /s.